

QUASI-SINGLE-MODE FIBER TRANSMISSION FOR SUBMARINE SYSTEMS

John D. Downie, William A. Wood, Jason Hurley, Michal Mlejnek, Ioannis Roudas, Aramais Zakharian, Snigdharaj Mishra (Corning Incorporated), Fatih Yaman, Shaoliang Zhang, Ezra Ip, Yue-Kai Huang (NEC Laboratories America)
Email: downiejd@corning.com

Corning Incorporated, 1 Riverfront Plaza, SP-AR-02-1, Corning, NY 14831, USA

Abstract: We investigate single-mode transmission over a few-mode optical fiber for submarine systems. The motivation is to achieve a larger effective area fiber with acceptable macrobend loss performance. While nonlinear impairments are lessened by larger fiber effective area, multi-path interference (MPI) becomes a new transmission issue that must be addressed. We model the growth of MPI in quasi-single-mode (QSM) transmission, measure MPI in spans of QSM fiber via different techniques, and present transmission results of high spectral efficiency systems over QSM fiber on link lengths representative of transoceanic distances.

1. INTRODUCTION

Given continued strong traffic growth in undersea networks, there is significant interest in increasing the total capacity in a single optical fiber over very long distances. In terms of optical fiber technology, the primary means to increasing capacity and/or reach are lower attenuation and nonlinear sensitivity, promoting higher achievable optical signal-to-noise ratio (OSNR). Nonlinear sensitivity is primarily governed by fiber effective area as well as material properties [1]. In practice, it can be difficult to make single-mode fibers with effective areas larger than approximately $150 \mu\text{m}^2$ without compromising bend loss performance. However, one means to increase the effective area and retain reasonable bend performance is to increase the cutoff wavelength, allowing the fiber to support another spatial mode. Relaxing a strict single-mode requirement allows larger effective areas, but also may introduce new impairments that must be addressed. Multi-path interference and excess loss

arising from mode coupling are two such impairments. In this paper we review and describe recent efforts in the area of single-mode transmission over few-mode fiber, or quasi-single-mode transmission. QSM transmission requires no changes to optical amplifiers and only potential changes to digital signal processing (DSP) in coherent receivers. We present modeling and measurement results that enable specifications to be set for mode coupling and differential mode attenuation (DMA). We also discuss MPI measurements for QSM fibers. Finally, we present experimental results for QSM transmission of 200 Gb/s channels over long distances with prototype fibers, and address DSP effectiveness for compensating MPI in the receiver.

2. FIBER FIGURE OF MERIT ANALYSIS FOR REPEATERED SYSTEMS

With the recent emergence of coherent receivers, the most important optical fiber parameters affecting long-haul and

submarine system performance for new systems are primarily attenuation and nonlinear tolerance. Chromatic dispersion can now be compensated through DSP in the digital coherent receiver, or divided between DSP functions in the transmitter and receiver. Digital dispersion compensation may also increase the nonlinear system performance compared to in-line dispersion compensation configurations [2,3]. Consequently, the measure of optical fiber for system performance is now largely the effective OSNR, governed by fiber attenuation and nonlinear tolerance.

Tailored to new coherent systems and specifically Nyquist wavelength division multiplexing (WDM), a generalized fiber figure of merit (FOM) has been developed based on the Gaussian noise model [4,5]. We employ a simplified version in Eq. 1, in which the FOM is defined relative to a reference fiber. Eq. 1 assumes equivalent chromatic dispersion for high-dispersion fibers such as those described by the ITU-T G.654 standard [6]. The amplifier noise figure is assumed to be constant, other loss components such as splice losses are ignored, and optimal launch power into each span is assumed for all fibers.

$$FOM(dB) = \frac{2}{3} \left(10 \log \left[\frac{A_{eff} \cdot n_{2,ref}}{A_{eff,ref} \cdot n_2} \right] - [\alpha_{dB} - \alpha_{ref,dB}] \cdot L - \frac{1}{3} \left(10 \log \left[\frac{L_{eff}}{L_{eff,ref}} \right] \right) \right) \quad (1)$$

In Eq. (1), A_{eff} is the effective area of the fiber under evaluation, n_2 is the nonlinear index of refraction, α_{dB} is the fiber attenuation in units of dB/km, L is the span length of the repeatered system being considered, and L_{eff} is the nonlinear effective length. The corresponding terms with “ref” in the subscript refer to the reference fiber. The effective interaction length L_{eff} [7] is approximately given by $1/\alpha$ for conventional span lengths, where α is the fiber attenuation in linear units km^{-1} .

As defined, the fiber FOM represents the difference in $20\log(Q)$ value between the fiber under evaluation and the reference fiber. The FOM results are shown in Fig. 1 for 80 km spans where the reference fiber has attenuation of 0.2 dB/km and A_{eff} of $80 \mu m^2$, approximating many standard single-mode fibers. Fig.1 clearly shows that reducing fiber attenuation and/or increasing effective area lead to increased FOM and better system performance. In Fig. 1, the discontinuity reflects an assumption that attenuation values below 0.175 dB/km are achieved with pure silica core fibers with lower nonlinear index n_2 compared to Ge-doped silica core fibers [1,6].

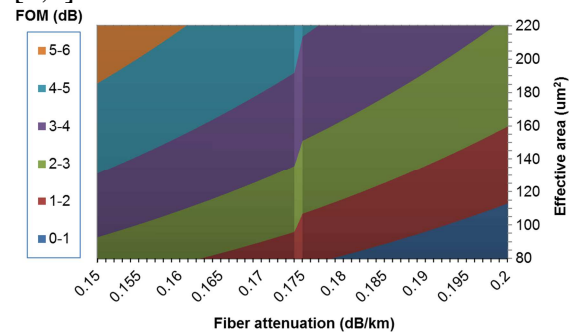


Fig. 1: Fiber FOM as function of attenuation and effective area for 80 km spans in repeatered systems.

Looking only at the effect of fiber A_{eff} , the change in FOM as a function of A_{eff} for constant attenuation is shown in Fig. 2. These results show that a fiber with A_{eff} of $150 \mu m^2$ compared to a fiber with A_{eff} of $100 \mu m^2$ has an increase in FOM of almost 1.2 dB. Moving from $150 \mu m^2$ to $200 \mu m^2$ brings more than 0.8 dB additional FOM improvement.

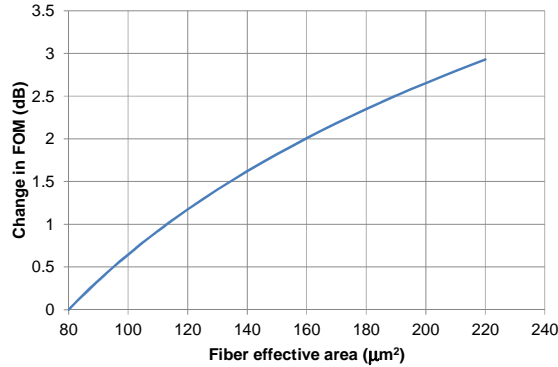


Fig. 2: Change in Fiber FOM as function of effective area for the same attenuation.

3. MODELING OF TRANSMISSION EFFECTS IN QUASI-SINGLE-MODE FIBER SYSTEMS

The FOM results in Figs. 1 and 2 assume that the fibers are single-mode fibers. As noted earlier, QSM fibers may offer a practical potential path toward larger fundamental mode A_{eff} . However, MPI can arise from mode coupling at splice points and in a distributed fashion during propagation. In this respect, QSM fibers may offer a trade-off of increased linear impairments for reduced nonlinear impairments. Such a trade-off may be worthwhile if MPI can be more easily compensated in DSP than nonlinear impairments.

A phenomenological model has been developed to predict the level of MPI generated by distributed mode coupling for quasi-single-mode transmission based on power coupled mode theory [8]. The model assumes that light is launched into only the fundamental LP_{01} mode of a fiber that supports two spatial modes. During propagation in the fiber, optical power will couple back and forth between the fundamental and higher order modes in a continuous fashion, governed by an average coupling constant κ (km^{-1}). At any point z in a fiber span, the optical power in the LP_{01} and LP_{11} modes can be

written as follows, assuming $P_{01}(0) = 1$, and $P_{11}(0) = 0$:

$$P_{01}(z) = \frac{1}{\delta} \left[\delta \cosh\left(\frac{\delta z}{2}\right) + \Delta\alpha \sinh\left(\frac{\delta z}{2}\right) \right] e^{-(\kappa+\alpha)z} \quad (2)$$

and

$$P_{11}(z) = \frac{2\kappa}{\delta} \sinh\left(\frac{\delta z}{2}\right) e^{-(\kappa+\alpha)z}, \quad (3)$$

where $\delta \equiv \sqrt{\Delta\alpha^2 + 4\kappa^2}$, $\Delta\alpha = \alpha_{11} - \alpha_{01}$ is the DMA in linear units, and $\alpha = (\alpha_{11} + \alpha_{01})/2$ is the average attenuation. With the definition of MPI as the ratio of crosstalk power to main signal power, we can write

$$MPI(z) = \frac{(P_{01}(z) - P_{\text{signal}}(z))}{P_{\text{signal}}(z)} \quad (4)$$

where $P_{\text{signal}}(z) = \exp[-(\alpha_{01} + \kappa)z]$ is the main signal power in the fundamental mode without any coupling back from the higher order mode. Using Eqs. 2 and 3, MPI can be written as

$$MPI(z) = \left[\cosh\left(\frac{\delta z}{2}\right) + \frac{\Delta\alpha}{\delta} \sinh\left(\frac{\delta z}{2}\right) \right] e^{-(\Delta\alpha \cdot z/2)} - 1 \quad (5)$$

or

$$MPI(z) \cong \frac{(\Delta\alpha \cdot z - 1 + e^{-\Delta\alpha z})}{\Delta\alpha^2} \kappa^2. \quad (6)$$

We note that Eq. 6 was also derived separately using a different approach [9]. Finally, we note the concept of excess loss (EL) for single-mode transmission in a two-mode fiber in comparison to a purely single-mode fiber with the same fundamental mode intrinsic attenuation α_{01} . Excess loss occurs because of the coupling out of the LP_{01} mode to the LP_{11} mode. Any power still in the LP_{11} mode at the end of a span will be lost as the two-mode fiber is spliced back into a single-mode fiber in the optical amplifier at the end of the span. Thus EL after a given distance can be defined as

$$EL(\text{dB}/\text{km}) = -10 \log \left[\frac{P_{01}(z)}{e^{-\alpha_{01}z}} \right] \frac{1}{z}. \quad (7)$$

From Eqs. 2-7, it is clear that the two main parameters that determine MPI and EL are the mode coupling coefficient κ and the

differential mode attenuation (DMA) $\Delta\alpha$. For EL, the dependence is almost entirely on the mode coupling coefficient, as shown in Fig. 3. For weak mode coupling, the EL is approximately 4.34κ (dB/km). On the other hand, both parameters are important in determining the MPI generated, as shown in Fig. 4. However, if the coupling coefficient could be made small enough (e.g. $\sim 1 \times 10^{-4} \text{ km}^{-1}$), then the DMA would be less significant in determining MPI.

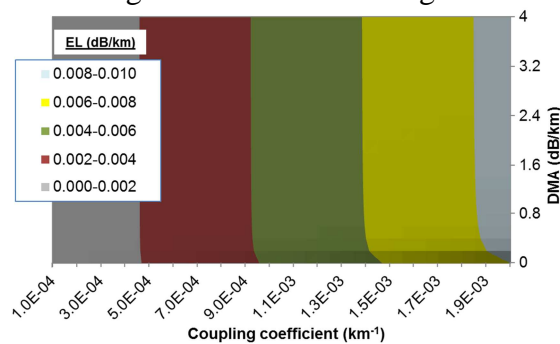


Fig. 3: Excess loss from mode coupling.

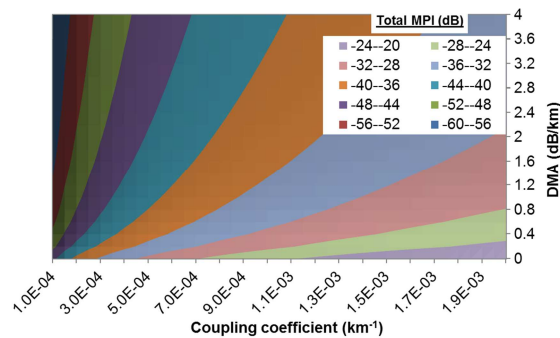


Fig. 4: MPI generated by distributed coupling in an 80 km span.

Besides the process of distributed mode coupling during propagation in the few-mode fiber, MPI can also be generated by mode coupling between the LP_{01} and LP_{11} modes at splice points within a span. To account for this contribution, we conservatively assume that a given splice loss α_{splice} (dB) of the fundamental mode results in all lost power being coupled to the LP_{11} mode, and similarly, any power already in the LP_{11} mode being coupled back to the LP_{01} mode with the same coupling strength. The discrete coupling strength is calculated as $\epsilon = 1 -$

$10^{(-\alpha_{splice}(dB)/10)}$. The effect of modeling the generated MPI in a span of 80 km as arising from both discrete splices and distributed mode coupling is illustrated in Fig. 5. The level of MPI generated as a function of distance into the 80 km span is shown for the cases with no splice losses and 0.02 dB splice loss occurring every 10 km in the span. For this figure, the distributed mode coupling coefficient was assumed to be 0.001 dB/km and the DMA was 2 dB/km. The splice loss of 0.02 dB between lengths of the few-mode fiber should be conservative for large effective area fibers such as those being considered here [6]. In this case, the inclusion of the splice losses increases the MPI at the end of the span by about 3 dB compared to a span with no internal splice-induced mode coupling events.

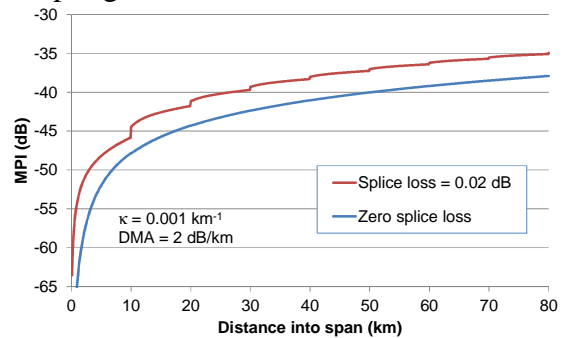


Fig. 5: MPI generated by both distributed and discrete mode coupling as a function of distance into an 80 km span.

The results from modeling analyses such as represented in Figures 3-5 can be used to help find specifications for the distributed mode coupling coefficient and the differential mode attenuation that will enable successful QSM fiber transmission. This also requires an estimate of the MPI level that can be tolerated and adequately compensated in receiver DSP. Toward that end, measurements were made of the Q penalty for varying levels of MPI for a 256 Gb/s PM-16QAM signal with and without receiver DSP MPI compensation [10]. The MPI compensation used a decision-

directed least-mean-squares (DD-LMS) equalizer with four filters in a butterfly configuration and 1001 symbol-spaced taps per filter. An example of some of the results from that study is shown in Fig. 6, given in terms of the Q penalty obtained after equalization relative to a signal with no MPI and no DD-LMS equalization. There were 8 independent crosstalk terms in the experiments with the total aggregate MPI given in the figure.

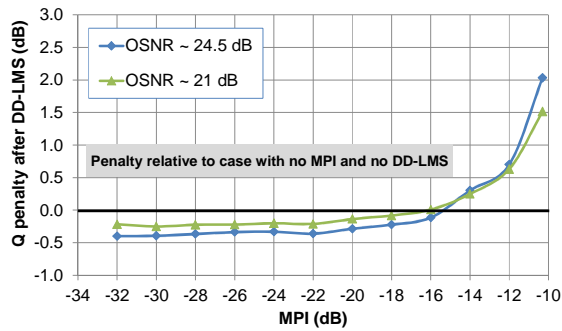


Fig. 6: Q penalty for a 256 Gb/s PM-16QAM signal after DD-LMS equalization relative to a signal with no MPI and no DD-LMS equalization.

No Q penalty was observed for total MPI values up to about -16 dB in this study. If we use this MPI level as a maximum threshold experienced by a PM-16QAM signal at the end of a transmission link, then we can reasonably estimate values of the mode coupling coefficient and DMA that will satisfy the threshold. For example, consider a link length of 7000 km comprised of 80 km spans. The total MPI at the end of the link will scale proportionally to the number of spans. To guarantee a total MPI of -16 dB or lower at the end of 7000 km, the MPI generated in a single 80 km span should be less than approximately -35 dB. The data in Fig. 5 suggests that this would be possible with a mode coupling coefficient of about 0.001 km^{-1} and a DMA value of about 2 dB/km, including MPI contributions from intra-span splices. If mode coupling from micro-bending can be reduced further, then

the requirement on DMA could also be relaxed.

4. MPI CHARACTERIZATION OF QSM FIBER SPANS

Given that MPI is a primary potential system impairment arising from QSM fiber transmission, it is important to accurately characterize the fiber to estimate the MPI generated during propagation in a span. There are a number of MPI estimation techniques that can be employed. In a direct approach, the OSNR penalty (compared to back-to-back transmission) at a given BER can be measured for linear transmission of a particular signal, and then compared to previously taken OSNR penalty data obtained for the same signal with well-known and calibrated levels of MPI generated with an MPI emulator [11]. Another approach involving transmission of a signal through the fiber in the linear regime assumes a Gaussian noise model of the MPI impairment [11,12]. In this approach, the multiple interferers arising from distributed mode coupling are modeled as Gaussian noise that acts in addition to ASE noise to create an effective OSNR that can be expressed as

$$OSNR_{eff} = \frac{P_{sig}}{P_{ASE} + P_{MPI,eq}} \quad (8)$$

where P_{sig} is the average signal power, P_{ASE} is the ASE noise power within the OSNR resolution bandwidth $\Delta\nu_{res}$, and $P_{MPI,eq}$ is the power of a fictitious additive white Gaussian noise, also within $\Delta\nu_{res}$, that produces the MPI penalty. The equivalent MPI noise term in Eq. 8 is obtained by scaling the total crosstalk power P_{xtalk} as $P_{MPI,eq} = P_{xtalk} \Delta\nu_{res}/B$, where B is the optical bandwidth of the signal determined by its spectrum and the receiver bandwidth. The crosstalk power is given by the definition of MPI as $MPI = P_{xtalk}/P_{sig}$. The level of MPI can then be determined from linear transmission

measurements of the signal through the fiber at given OSNR levels by

$$MPI = (B/\Delta v_{res}) [OSNR_{eff}^{-1} - OSNR_{ASE}^{-1}] . \quad (9)$$

As illustrated in Fig. 7 with a hypothetical example, $OSNR_{ASE}$ is the actual measured OSNR of the system with MPI that produces a given BER value, and $OSNR_{eff}$ is the effective OSNR corresponding to the OSNR value required of that signal in back-to-back transmission in the absence of MPI to achieve the same BER.

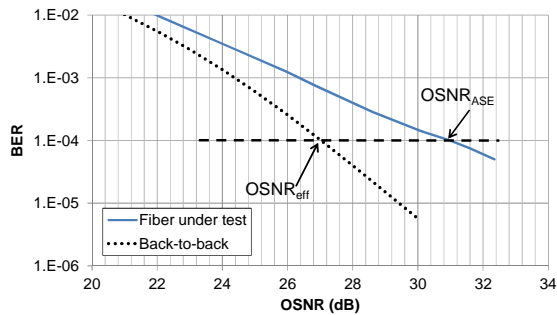


Fig. 7: Example of definitions of $OSNR_{ASE}$ and $OSNR_{eff}$ for MPI estimation using Gaussian noise model.

Another MPI measurement approach we have used to estimate the MPI generated in a few-mode fiber for QSM transmission involves launching a CW laser into the fiber and evaluating the power fluctuations of the laser at the output of the span [11,13]. The laser is launched into the fundamental mode, and then only the power contained in the fundamental mode is detected, by stripping out the LP_{11} mode at the span end. The laser linewidth was comparable to the transmission lasers used for the previous technique, the detector averaging time was 20 ms, a polarization scrambler was used at the launch end, and power measurements were obtained every 0.25 sec for at least 2 hours. The measurements are analyzed to determine MPI according to

$$MPI(dB) = 20 \log[\sigma/P_{ave}], \quad (10)$$

where P_{ave} is the average received power of the detected laser after propagation through

the fiber and σ is the standard deviation of the power [12].

Some results for MPI estimates of few-mode fiber spans used for QSM transmission are shown in Fig. 8, comparing the three described measurement approaches. The estimates obtained were very similar with the different methods. The data were for two low-MPI spans of length 154 km, and an 89 km span made from a different fiber with higher MPI.

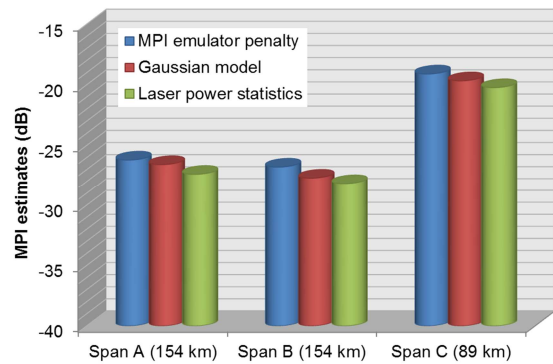


Fig. 8: MPI estimates of three few-mode fiber spans using different methods.

5. TRANSMISSION EXPERIMENTS AND RESULTS

There have been relatively few transmission experiments with single-mode transmission over few-mode fibers. In an early experiment, significantly increased reach for 100 Gb/s PM-QPSK signals was reported by virtue of the few-mode fiber's larger effective area [14]. No significant MPI impact was observed in that experiment. Compensation of MPI from QSM transmission in receiver DSP was proposed first [15], and then demonstrated experimentally for the first time in which the DSP increased the reach of 200 Gb/s PM-16QAM signals by more than a factor of two, with a total reach of 2600 km [16]. Most recently, transmission experiments with high spectral efficiency (6.5 bits/s/Hz) have been carried out that demonstrate the performance advantages of both hybrid

fiber spans and multi-subcarrier modulation formats for QSM fiber systems [17].

In [17], the transmission system spans of length 101.6 km were comprised of 51.3 km of few-mode fiber followed by 50.3 km of Vascade[®] EX3000 fiber, a large effective area single-mode fiber. This type of span construction achieved a higher system nonlinear tolerance from the few-mode fiber with effective area of approximately $200 \mu\text{m}^2$, but reduced the total MPI by shortening the total length of few-mode fiber used in the link. Similarly, the use of a novel modulation format with 32 subcarriers at 1 Gbaud symbol rate significantly reduced the number of taps required per subcarrier in the equalizer for MPI compensation. This resulted in increased equalizer effectiveness compared to a single carrier 32 Gbaud modulation format. The difference in performance between the single carrier and multi-subcarriers formats is illustrated in Figs. 9 and 10, with Q given vs. number of taps in the DD-LMS equalizer for two transmission distances. While the DD-LMS equalization is highly effective for the single carrier format at 4060 km, that format is no longer compensated well at 6600 km, even with 1001 taps or more. On the other hand, the multi-subcarrier format requires about 101 taps per subcarrier in either the normal CMA equalizer or the optional subsequent DD-LMS equalizer. In fact, the data in Fig. 10 shows that with 101 taps in the CMA equalizer, the DD-LMS equalizer is unnecessary. Furthermore, the multi-subcarrier format enabled a significantly longer reach overall.

A direct comparison of the transmission performance between the hybrid span construction and homogeneous spans comprised of either fiber is shown in Fig. 11 for the multi-subcarrier format. The hybrid span had the best performance

because of its larger A_{eff} than the single-mode fiber and its reduced MPI impact compared to the all-few-mode fiber system.

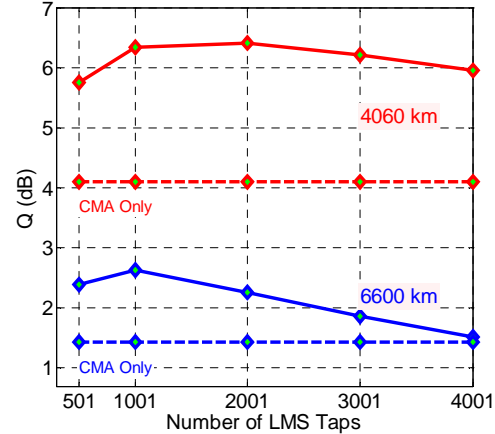


Fig. 9: Q vs. number of DD-LMS taps for single carrier PM-16QAM modulation format.

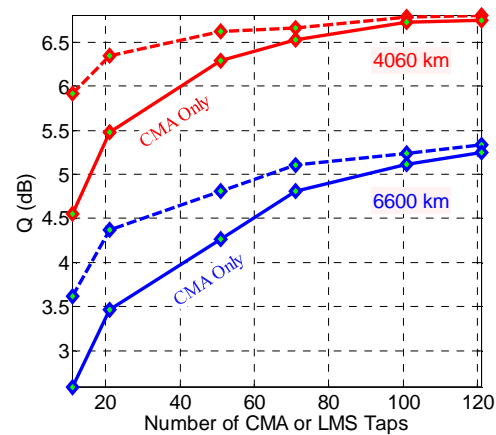


Fig. 10: Q vs. number of CMA or DD-LMS taps per subcarrier for multi-subcarrier modulation format.

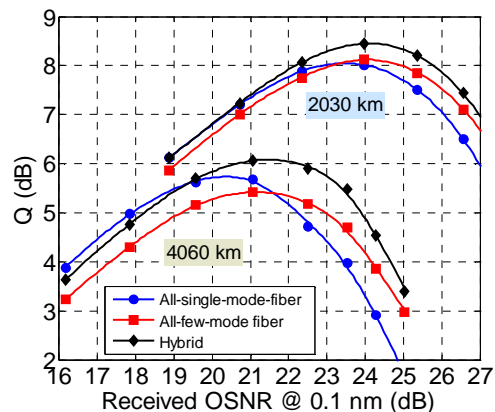


Fig. 11: Q vs. received OSNR for multi-subcarrier modulation format with different system span constructions.

6. SUMMARY

We have examined some of the issues and trade-offs involved with single-mode transmission over few-mode fiber for submarine systems. MPI becomes a linear impairment to be addressed that is essentially substituted for nonlinear impairments. We reviewed experimental transmission results over 6600 km that demonstrated better performance with a hybrid span configuration than with a purely single-mode fiber system.

7. REFERENCES

- [1] K. S. Kim *et al*, "Measurement of the nonlinear index of silica-core and dispersion-shifted fibers," *Opt. Lett.* vol. **19**, pp. 257-259, 1994.
- [2] K. Roberts *et al*, "Performance of Dual-Polarization QPSK for Optical Transport Systems," *J. of Lightwave Tech.*, vol. **27**, pp.3546-3559, August 2009.
- [3] A. Bononi *et al*, "Which is the Dominant Nonlinearity in Long-haul PDM-QPSK Coherent Transmissions?," in *Proc. of European Conf. Opt. Commun.* (2010), paper Th.10.E.1.
- [4] V. Curri *et al*, "Fiber figure of merit based on maximum reach," OFC/NFOEC 2013, paper OTh3G.2, (2013).
- [5] M. Hirano *et al*, "Record Low Loss, Record High FOM Optical Fiber with Manufacturable Process," OFC/NFOEC 2013, paper PDP5A.7, (2013).
- [6] S. Makovejs *et al*, "Towards Superior Transmission Performance in Submarine Systems: Leveraging Ultra-Low Attenuation and Large Effective Area," *J. Lightwave Tech.*, to be published in Feb. 2016.
- [7] G.P. Agrawal, *Nonlinear Fiber Optics*, San Diego, CA: Academic Press, 1989.
- [8] M. Mlejnek *et al*, "Coupled-Mode Theory of Multipath Interference in Quasi-Single Mode Fibers," *IEEE Photonics J.*, vol. **7**, no. 1, article #7100116 (2015).
- [9] Q. Sui *et al*, "Long-haul Quasi-Single-Mode Transmissions using Few-Mode Fiber in presence of Multi-Path Interference," *Opt. Express* vol. **23**, issue 3, 3156-3169 (2015).
- [10] J. D. Downie *et al*, "Assessment of MPI compensation effectiveness as functions of MPI level and number of crosstalk terms for a 256 Gb/s PM-16QAM signal," SPPCom 2015, Boston MA, June 2015, Paper SpS4D.4, (2015).
- [11] J. D. Downie *et al*, "MPI measurements of quasi-single-mode fibers," in *IEEE Photonics Conference (IPC) 2015*, Reston, VA, October 2015, pp. 273-274, paper MG3.4, (2015).
- [12] W. Zheng *et al*, "Measurement and System Impact of Multipath Interference From Dispersion Compensating Fiber Modules," *IEEE Trans. on Instrum. and Meas.*, vol. **53**, pp. 15-23 (2004).
- [13] S. Ramachandran *et al*, "Measurement of Multipath Interference in the Coherent Crosstalk Regime," *IEEE Photon. Technol. Lett.*, vol. **15**, pp. 1171-1173 (2003).
- [14] F. Yaman *et al.*, "10x112Gb/s PDM-QPSK transmission over 5032 km in few-mode fibers," *Optics Express* vol. **18**, pp. 21342-21349 (2010).
- [15] N. Bai, C. Xia, and G. Li "Adaptive frequency-domain equalization for the transmission of the fundamental mode in a few-mode fiber," *Opt. Express* vol. **20**, pp. 24010-24017 (2012)
- [16] Q. Sui *et al*, "256 Gb/s PM-16-QAM Quasi-Single-Mode Transmission over 2600 km using Few-Mode Fiber with Multi-Path Interference Compensation," OFC 2014, paper M3C.5 (2014).
- [17] F. Yaman *et al*, "First Quasi-Single-Mode Transmission over Transoceanic Distance using Few-mode Fibers," OFC 2015, Los Angeles, CA, Postdeadline paper Th5C.7, (2015).